R. & M. No. 2663
(11,291)
A.R.C. Technical Report

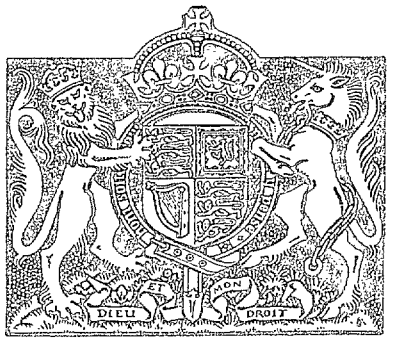

MINISTRY OF SUPPLY

AERONAUTICAL RESEARCH COUNCIL
REPORTS AND MEMORANDA

The Effect of Spanwise Rib-boom Stiffness on the Stress Distribution near a Wing Cut-out

By

E. H. MANSFIELD, B.A.

LONDON : HER MAJESTY'S STATIONERY OFFICE
1952

SIX SHILLINGS NET

The Effect of Spanwise Rib-boom Stiffness on the Stress Distribution near a Wing Cut-out

By

E. H. MANSFIELD, B.A.

COMMUNICATED BY THE PRINCIPAL DIRECTOR OF SCIENTIFIC RESEARCH (AIR), MINISTRY OF SUPPLY

*Reports and Memoranda No. 2663**

December, 1947

Summary.—A theoretical investigation is made into the effect of spanwise rib-boom stiffness on the stress distribution at a cut-out in the inter-spar skin of a stressed skin wing in bending. Both shear and bending stiffness of the rib-boom are taken into account, and attention is concentrated on the case in which the rib-boom is built-in to the spar flanges.

Curves are included which determine, for any particular case, the magnitude of the peak shear stress adjacent to the flange, the approximate spanwise variation of this shear stress, the proportion of load transferred by the rib-boom to the skin and stringers, and the bending moment in the rib-boom at its points of attachment to the spar flanges.

By suitable design of the rib-boom it is possible to lower the shear stresses adjacent to the flange with little or no increase in structure weight.

Available experimental results for the peak shear stresses are in good agreement with this theoretical work; previously developed methods[1, 3] give over-estimates of the order of 100 per cent.

1. *Introduction.*—In the neighbourhood of a cut-out in the interspar region of a stressed-skin wing the end load due to bending is carried almost entirely by the spar flanges. Beyond the cut-out, however, the sheet, by virtue of its shear stiffness, distributes this end load so that it is eventually taken uniformly by the sheet, stringers and flanges. This is a common load diffusion problem which has been considered by a number of writers[1, 3]. The effect of a chordwise rib-boom attached to the sheet at the end of the cut-out is ignored by these writers (in any practical case there will be such a boom), and the maximum shear stresses predicted are accordingly too high, in some cases being two or three times those given by available experimental results.

The purpose of this report is to investigate theoretically the effect of such a rib-boom on the stress distribution and in particular on the shear stresses.

2. *Statement of Problem and Assumptions.*—The problem is to determine the stress distribution in a long rectangular stiffened panel (length greater than twice width) which is bounded on its longer edges by equal flanges of constant cross-section to which are applied equal direct loads. A rib-boom is attached to the skin at the end of the cut-out and is regarded as a beam of constant section; attention is concentrated on the case in which the rib-boom is built-in to the spar flanges, as this is closely representative of current practice; both shear and bending stiffnesses of the rib-boom are taken into account.

* R.A.E. Report Structures 13, received 21st February, 1948.

The stringer-sheet method[1, 2, 3] is used, and curvature of the surface is neglected. Any rotation of the spar flanges in the plane of the panel is ignored though this effect (due to bending flexibility of the flanges) is considered approximately in Appendix II.

3. *Discussion.*—The presence of a rib-boom has an important effect on the stress distribution, especially on the shear stress adjacent to the spar flanges ; if the rib-boom is ignored the shear stresses have a very high value at the end of the cut-out—the stringer-sheet method of solution giving an infinite value and the finite-stringer method giving a value depending critically on the stringer pitch.

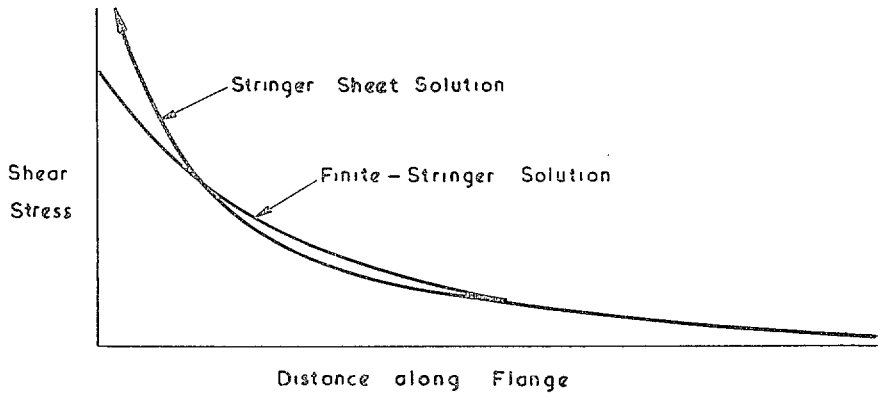

DIAG. 1. Shear Stress adjacent to the spar flange (no rib-boom).

The effect of a rib-boom can be estimated by regarding it as a beam in bending ; if the beam is built-in at each end to the spar flanges its rotation will be zero and hence, if we neglect the shear flexibility of the beam, the shear stress in the sheet adjacant to the spar flange will also be zero to start with. Except for rib-booms with high bending stiffness the effect of a rib-boom is comparatively localised and the shear stress adjacent to the spar-flanges increases rapidly to a maximum value, and then dies away in much the same way as if there were no rib-boom.

If the shear stiffness of the rib-boom is taken into account the shear in the sheet will have a finite value at the root and the distribution will be roughly as shown by the broken line in Diag. 2.

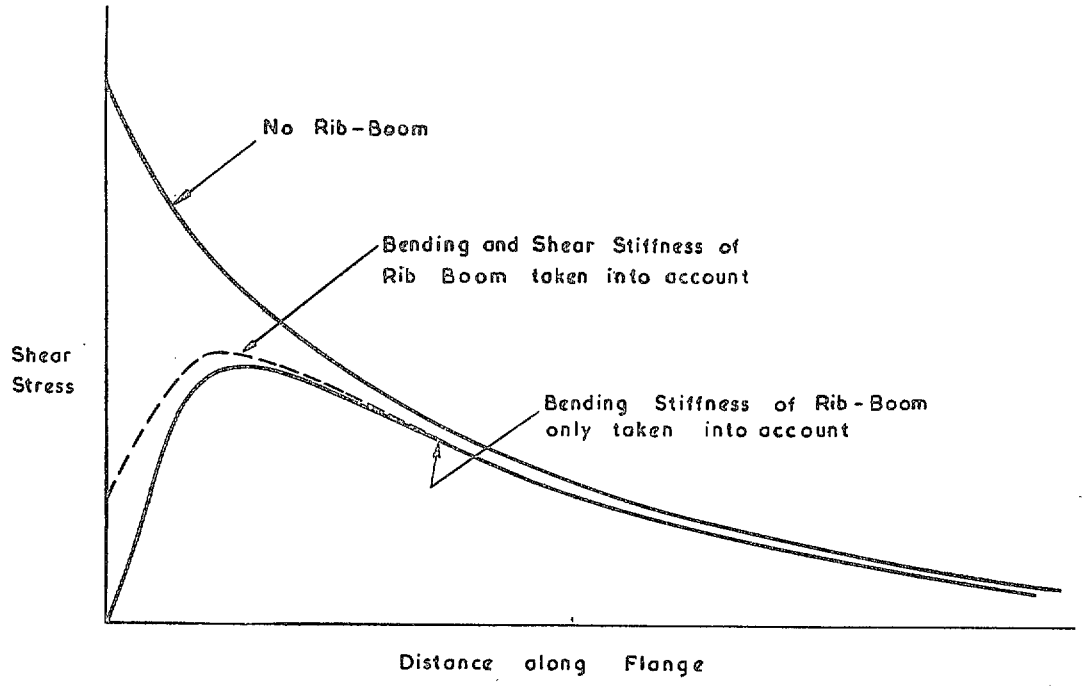

DIAG. 2. Shear stress adjacent to spar flange (with rib-boom).

If the rib-boom is not rigidly built-in to the spar flanges but is intermediate between the simply-supported and built-in case the effect on the stress distribution will be similar to that of a decrease in the shear stiffness of the rib-boom, and this, though marked at the root, does not appreciably affect the peak shear stresses.

4. *Description of Results* (For symbols *see* page 7).—Unless otherwise stated the rib-boom is built-in at its ends.

The complete stress distribution is shown to depend primarily on three non-dimensional parameters, α, β, γ. It is therefore impracticable to present the results in such a way as to cope with all possible types of structure dimensions; however, it is shown that the effect of γ (which depends on the shear stiffness of the rib-boom) is not important so unless otherwise stated γ has been assumed zero and the results have been plotted for various α and β. A few curves in which γ is non-zero are given to show the general effect of this parameter. (α is the proportion of flange area to stringer-sheet area and β is proportional to the bending stiffness of the rib-boom.)

4.1 *Shear Stress Adjacent to the Spar Flanges.*—A family of curves in which $\alpha = 1$ (*i.e.*, flange area = stringer-sheet area) has been drawn in Fig. 1 for a wide range of β (the range covers the practical range) showing the variation of shear stress adjacent to the spar flanges; and in Fig. 2 similar curves have been drawn including the effect of the shear stiffness of the rib-boom: γ has been taken to be given by—

$$\gamma = 0{\cdot}04\,\beta^{1/2};$$

the reason for this being that for a given *shape* of rib-boom cross-section $\beta \propto l^4$ and $\gamma \propto l^2$ where l is a typical dimension, and hence $\gamma \propto \beta^{1/2}$ provided the sectional shape of the rib-boom is unaltered. The constant, $0{\cdot}04$, is typical of current practice.

The variation of shear stress for a particular value of β (*i.e.*, a given rib-boom) for various values of α is shown in Fig. 3. If the flange load is kept constant the effect of increasing the flange area is to lower the shear stresses and to move the position of the peak shear stress slightly further from the rib-boom. If the flange stress is kept constant the effect of increasing the flange area is to increase the sheer stresses.

The effect of varying the shear stiffness of the rib-boom is shown in Fig. 4, where $\alpha = 1$ and $\beta = 2 \times 10^{-4}$ and γ has the three values: $0{\cdot}02\,\beta^{1/2}$, $0{\cdot}04\,\beta^{1/2}$, $0{\cdot}08\,\beta^{1/2}$. The effect is pronounced at the root though the increase to the peak shear stress is not important. The largest value of γ chosen here is unlikely to occur in practice, and it will usually be sufficient to ignore this effect altogether. The value of the shear stress at the root may be obtained closely, but indirectly, from Fig. 7 (*see* section 5.4) where the proportion of end load transferred by the rib-boom is given. This proportion, δ, say, is practically independent of γ and hence the shear load in the rib-boom adjacent to the flange will be approximately $\delta f_0 F$. This makes the shear stress in the rib-boom $\delta f_0 F/R$ which must also be the shear stress in the sheet adjacent to the rib-boom.

4.2 *Maximum Shear Stress Adjacent to the Spar Flanges.*—The value of the peak shear stress adjacent to the spar flange is of practical importance and these peak values can be obtained from Fig. 5 for any values of the parameters α and β. The effect of the shear stiffness of the rib-boom has been included for the case in which $\alpha = 1$; γ has again been taken to be $0{\cdot}04\,\beta^{1/2}$. The case when the rib-boom is simply-supported has also been shown.

4.3 *Direct Stress in the Spar Flanges.*—The distribution of direct stress in the spar flanges is given in Fig. 6 for various values of β. Except for comparatively stiff rib-booms the distribution is much the same as if there were no rib-boom. This means that simplified theories, such as that of Ref. 1 may be used to estimate the direct stress in the flanges.

4.4 *Proportion of End Load Transferred by the Rib-boom.*—Due to the stiffness of the rib-boom a proportion of the total end load is transferred immediately by the rib-boom to the sheet and stringers. This proportion is seldom more than 20 per cent and there is a corresponding decrease

in the spar flange stress just inboard of the rib. The effect of ignoring the shear flexibility of the rib-boom is very small as will be seen from Fig. 7 where the proportion of end load is plotted for various α and β with γ zero and for a particular γ $(= 0{\cdot}04\,\beta^{1/2})$ when $\alpha = 1$.

It will be noticed that over the practical range the proportion of load transferred by the rib-boom is roughly proportional to $\beta^{1/4}$, *i.e.*, to the linear size of the rib-boom cross-section.

The proportion of end load transferred by the rib-boom may be related to the maximum possible load that could be transferred by observing that when the rib-boom is infinitely stiff this proportion is $1/(1 + \alpha)$.

4.5 *Bending Moment in the Rib-boom at its Ends.*—The bending moment in the rib-boom at its points of attachment to the spar flanges is an important factor for two reasons; it is the greatest bending moment in the rib-boom and may therefore be a deciding factor in the design of the boom, and it will partly decide the strength of the rib-boom-to-flange attachment. It will be remembered, though, that one of the assumptions made was that the flanges remained straight. In practice, the flange will rotate slightly and relieve the end bending moment. This is considered in Appendix II.

The bending moment is expressed in terms of $f_0a^2t_s$ in Fig. 8. The line $\alpha = \infty$ drawn there corresponds to the case of constant stress flanges.

The effect of the shear flexibility of the rib-boom is again very small.

If we denote the bending moment (M, say) expressed as a fraction of $f_0a^2t_s$ by Δ (*i.e.*, Δ is the ordinate in Fig. 8), it is worth noting that for the rib-boom

$$\frac{M}{I} = \frac{\Delta k f_0}{a\beta}$$

and, as Δ is roughly proportional to $\beta^{3/5}$ over the practical range, it follows that for rib-booms of similar section the maximum stress in the rib-boom varies approximately as (a typical dimension)$^{-3/5}$.

5. *Agreement with Experiment.*—Experimental results have been obtained from strain-gauge readings taken during tests of four aircraft components, all of conventional monocoque construction. The values of the peak shear stress adjacent to the flange were found in each case and have been plotted in Fig. 9a. It will be seen that agreement with theory is good—in each case the theoretical value exceeding the experimental value by about 10 per cent. The previously developed approximate methods[1,3] gave overestimates of about 100 per cent.

In one case, there was considerable camber of the skin between the flanges and an estimate was made of an equivalent flat skin width; a small change in this estimate made little difference to the corresponding theoretical peak shear stress.

In Fig. 9b a number of experimental points showing the distribution of shear stress adjacent to the flange is given and agreement is again good, though in the actual structure the flange area decreased in a number of steps and the experimental points at some distance from the rib-boom have been factored to account for this. In practice, of course, the important thing to know will be the value of the peak shear stress likely to be developed and its approximate position.

6. *Example.*—The following dimensions specify the structure, which is representative of a large aircraft wing.

The position of this peak, obtained approximately from Fig. 1, will be $0{\cdot}05 \times ak$, i.e., 5 in., from the rib-boom. It will be further noticed that the shear stresses are appreciable (80 per cent of the maximum value) up to a distance of 15 in. from the rib-boom.

The proportion of load transferred immediately to the skin and stringers is found from Fig. 7 to be 13 per cent. This means that the direct stress in the flange just inboard of the rib-boom will be $0{\cdot}87 f_0$.

The shear stress in the rib-boom at its ends, which is also the shear stress in the sheet at the rib-boom flange junction, is

$$\frac{0{\cdot}13 \times f_0 \times 4}{1{\cdot}5} = 0{\cdot}35 f_0.$$

The bending moment in the rib-boom at its points of attachment to the spar flanges is given in Fig. 8 where we have

$$\begin{aligned} M &= 0{\cdot}008 f_0 a^2 t_s \\ &= 1{\cdot}6 f_0 , \end{aligned}$$

which implies a maximum bending stress in the rib-boom of

$$\begin{aligned} &\frac{1{\cdot}4 \times 1{\cdot}6 f_0}{1{\cdot}5}, \left(i.e., p = \frac{My}{I}\right) \\ &= 1{\cdot}5 f_0 . \end{aligned}$$

If we wish to limit this stress to f_0 (in practice this stress will tend to relieve itself due to rotation of the flanges. *See* Appendix II) we might increase the linear size of the rib-boom in the ratio $(1{\cdot}5 : 1)^{5/3}$, a result which follows from Section 4.5. This means nearly doubling the size of the rib-boom; but this is clearly an inefficient way, from the weight of view, of distributing the structure material, for that part of the rib-boom in the centre region of the panel does little work in relieving the high stresses at the ends of the rib-boom. A far more efficient scheme would be to have a tapering rib-boom with a moment of inertia at each end designed to take the original maximum bending load (*i.e.*, $1{\cdot}6 f_0$) and tapering to a much smaller value so as not to increase this moment. Such a scheme would suggest an I at each end of

$$I_0 \times \left(\frac{1{\cdot}5 f_0}{f_0}\right)^{1/3} = 1{\cdot}7 \text{ in.}^4$$

tapering to a value in the centre of, say, $0{\cdot}8$ in.^{4}

7. *Conclusions.*—By taking account of the spanwise stiffness of the rib-boom, an accurate estimate can be made of the stress distribution near a cut-out in the interspar skin of a stressed-skin wing. The previously developed methods (in which the rib-boom is ignored) give much the same values for the direct stresses in the spar flanges but overestimate the peak shear stresses in the sheet by a wide margin.

Curves are included for determining the shear stresses in the sheet and the principal loads in the rib-boom.

The method of analysis given in the Appendix lends itself readily to the solution of problems of this type[5], though some of the series involved converge very slowly.

LIST OF SYMBOLS

$2a$ Width of panel

t Thickness of sheet

t_s Thickness of stringer-sheet

F Area of each flange

I Moment of inertia of rib-boom (bending about a line perpendicular to the plane of the sheet)

R Effective area of rib-boom (for estimating its shear stiffness)

E, G Elastic moduli

f_0 Direct stress in flanges at rib (*i.e.*, stress applied to flanges)

$k = Et_s/Gt$
$\alpha = F/at_s$
$\beta = kI/a^3 t_s$
$\gamma = EI/GRa^2$
} Non-dimensional parameters

Additional symbols for use in Appendix 1

f_1 Direct stress in spar flanges immediately adjacent to rib on the side of the rib attached to the skin

f Uniform direct stress in the flanges and sheet at a considerable distance from the rib

σ Direct stress in sheet parallel to length of panel

τ Shear stress in sheet

u Displacement parallel to length of panel

x Co-ordinate measured along length of panel

y Co-ordinate measured normal to length of panel

Suffices F and R refer to the flanges and rib respectively

Suffices x and y denote differentiation with respect to the variable

---

REFERENCES

No.	*Author*	*Title, etc.*
1	M. Fine and H. G. Hopkins ..	Stress Diffusion Adjacent to Gaps in the Interspar Skin of a Stressed-Skin Wing. A.R.C. 5941. May, 1942. (To be published.)
2	D. Williams, R. D. Starkey and R. H. Taylor.	Distribution of Stress Between Spar Flanges and Stringers for a Wing under Distributed Loading. R. & M. 2098. June, 1939.
3	J. Hadji-Argyris	Diffusion of Symmetrical Loads into Stiffened Parallel Panels with Constant Area Edge Members. R. & M. 2038. November, 1944.
4	M. Fine	A Comparison Between Plain and Stringer-reinforced Sheet from the Shear Lag Standpoint. A.R.C. 5455. October, 1941. (To published.)
5	E. H. Mansfield	Generalised Fourier Series and the Roots of the Governing Transcendental Equations. R.A.E. Report No. Structures 12. December, 1947. (To be published.)

APPENDIX I

Details of Analysis

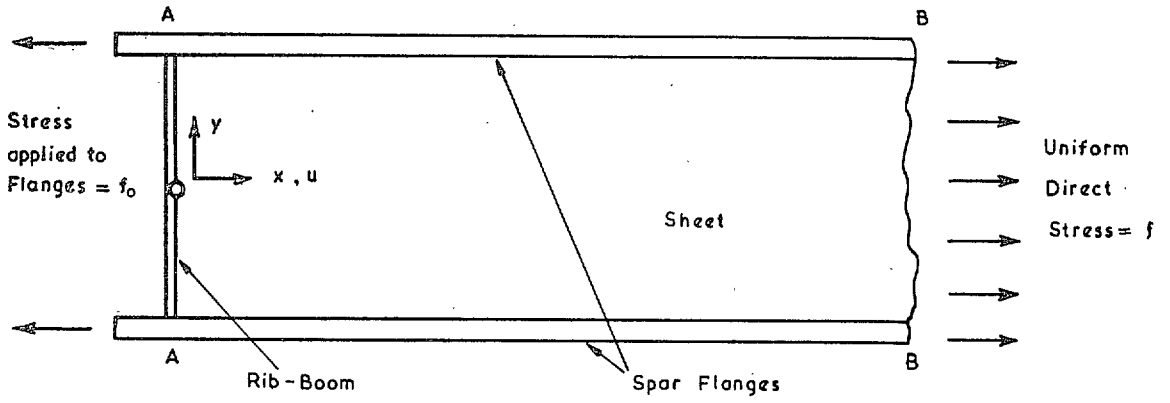

DIAG. 4

The notation is given on the previous page and the above diagram shows the general layout. The panel is taken to be indefinitely long but for practical purposes it is sufficient if the length of the panel is greater than about twice its width. At section AA the spar flanges are subject to a stress f_0 ; across a section BB, sufficiently far from AA, the stress distribution is uniform, the direct stress in the flanges and the sheet being $f = f_0(1 + at_S/F)^{-1}$ and the shear stress zero.

The longitudinal displacement (u) of the sheet satisfies the equation[1],

$$u_{xx} + \left(\frac{1}{k^2}\right) u_{yy} = 0\,,\; k^2 = \frac{Et_s}{Gt}\,, \qquad \ldots\ \ldots\ \ldots\ \ldots\ \ldots\ \ldots \quad (1)$$

where a suffix denotes differentation with respect to the variable ; the direct and shear stresses are given by

$$\sigma = Eu_x \quad \text{and} \quad \tau = Gu_y\,. \qquad \ldots\ \ldots\ \ldots\ \ldots\ \ldots \quad (2)$$

The most general solution of equation (1) satisfying

$$\text{(i)}\ \ u = 0 \text{ at } x = 0, y = \pm a,$$
$$\text{(ii)}\ \ u(y) = u(-y),\ -a \leqslant y \leqslant a\,,$$
$$\text{(iii)}\ \ (\sigma)_{x=\infty} = (Eu_x)_{x=\infty} = f\,,\ -a \leqslant y \leqslant a\,,$$

and

$$\text{(iv)}\ \ (\tau)_{x=\infty} = (Gu_y)_{x=\infty} = 0\,,\ -a \leqslant y \leqslant a\,,$$

is

$$Eu = fx + akf\,\Sigma\, A_n\left\{\exp\left(\frac{-r_n x}{ak}\right)\cos\left(\frac{r_n y}{a}\right) - \cos r_n\right\} \qquad \ldots\ \ldots\ \ldots \quad (3)$$

where the A_n and r_n are to be found from the equilibrium of the flanges and the rib-boom, and the continuity of displacements of the sheet, flanges and rib-boom.

For the equilibrium of the flanges we have

$$EF\,(u_F)_{xx} = t\tau\,, \quad y = \pm a$$
$$= tGu_y\,,\ y = \pm a$$

$$= \frac{-tGkf}{E} \Sigma A_n r_n \sin r_n \exp \frac{-r_n x}{ak}, \quad .. \quad .. \quad .. \quad .. \quad .. \quad (4)$$

and the solution of equation (4) satisfying

$$\text{(i)} \quad u_F = 0, \quad x = 0$$
$$\text{(ii)} \quad Eu_{Fx} = f_1, \quad x = 0$$

and

$$\text{(iii)} \quad Eu_{Fx} = f, \quad x = \infty$$

is

$$EFu_F = Ff_1 x + fat_s \Sigma A_n \sin r_n \left[\frac{ak}{r_n}\left\{1 - \exp\left(\frac{-r_n x}{ak}\right)\right\} - x\right] \quad .. \quad .. \quad .. \quad (5)$$

where

$$f_1 = f + \frac{fat_s}{F} \Sigma A_n \sin r_n .$$

The displacement of the flange is the same as the displacement of the edge of the sheet and hence, from equations (3) and (5), it is found that the r_n's satisfy the equation

$$\tan r_n = \frac{-Fr_n}{at_s}$$
$$= -\alpha r_n . \quad .. \quad .. \quad .. \quad .. \quad .. \quad .. \quad .. \quad .. \quad .. \quad (6)$$

The summations in the equations, therefore, extend over all positive values[5] of r_n satisfying equation (6).

In considering the equilibrium of the rib-boom it is convenient to regard the rib-boom displacement u_R as being made up of two parts, $u_R{}^b$ due to bending and $u_R{}^s$ due to shear displacement. We can then write

$$\left.\begin{aligned} (u_R{}^b)_{yyyy} &= \frac{\sigma t_s}{EI} \\ (u_R{}^s)_{yy} &= \frac{-\sigma t_s}{GR} \end{aligned}\right\} \text{at } x = 0 \quad .. \quad .. \quad .. \quad .. \quad .. \quad .. \quad (7)$$

and from equation (3) we have

$$(\sigma)_{x=0} = f\left\{1 - \Sigma A_n r_n \cos\left(\frac{r_n y}{a}\right)\right\} . \quad .. \quad .. \quad .. \quad .. \quad .. \quad .. \quad (8)$$

Substituting equation (8) in (7) and integrating gives

$$u_R{}^b = \frac{ft_s}{EI}\left\{\frac{y^4 - a^4}{24} + Ca^2(y^2 - a^2) - a^4 \Sigma \frac{A_n}{r_n^3}\left[\cos\left(\frac{r_n y}{a}\right) - \cos r_n\right]\right\} \quad .. \quad .. \quad (9)$$

where C is a constant determined by the end fixity of the rib-boom,

$$u_R{}^s = \frac{-ft_s}{GR}\left\{\frac{y^2 - a^2}{2} + a^2 \Sigma \frac{A_n}{r_n}\left[\cos\left(\frac{r_n y}{a}\right) - \cos r_n\right]\right\} . \quad .. \quad .. \quad .. \quad (10)$$

If the rib-boom is built-in at $y = \pm a$:

$$(u_R{}^b)_y = 0 \quad \text{at} \quad y = \pm a$$

and hence

$$-C = \frac{1}{12} - \frac{\alpha}{2}\Sigma\frac{A_n}{r_n}\cos r_n; \qquad \ldots\ldots\ldots\ldots\ldots\ldots\ldots \quad (11)$$

and if the rib-boom is simply-supported

$$(u_R^b)_{yy} = 0 \quad \text{at} \quad y = \pm a:$$

$$i.e., \quad -C = \tfrac{1}{4} + \tfrac{1}{2}\Sigma\frac{A_n}{r_n}\cos r_n . \qquad \ldots\ldots\ldots\ldots\ldots\ldots \quad (12)$$

The displacement of the rib-boom is the same as the displacement of the edge of the sheet, and as the rib-boom and sheet displacements are already zero at $x = 0$, $y = \pm a$, this will be the case if

$$(u_R)_y \equiv (u_R^b)_y + (u_R^s)_y$$

$$= u_y \quad \text{at} \quad x = 0, \quad -a \leqslant y \leqslant a.$$

$$i.e., \quad -k\Sigma A_n r_n \sin\left(\frac{r_n y}{a}\right) = \frac{t_s}{I}\left\{\frac{y^3}{6} + 2a^2yC + a^3\Sigma\frac{A_n}{r_n^2}\sin\left(\frac{r_n y}{a}\right)\right\}$$

$$- \frac{Et_s}{GR}\left\{y - a\Sigma A_n \sin\left(\frac{r_n y}{a}\right)\right\}. \qquad \ldots\ldots \quad (13)$$

The integral

$$\int_0^a \sin\left(\frac{r_n y}{a}\right)\sin\left(\frac{r_m y}{a}\right)dy$$

has the value

$$\frac{a(1 + \alpha\cos^2 r_n)}{2}$$

if $m = n$, and is otherwise zero. Using this relation, we obtain from equation (13)

$$A_n = \frac{-\sin r_n}{\alpha D_n}\left\{4(1 + \alpha)\left(C - \frac{\gamma}{2}\right) + \frac{1}{3} + \alpha - \frac{2(1 + \alpha)}{r_n^2}\right\} \qquad \ldots\ldots \quad (14)$$

where

$$D_n = (1 + \alpha\cos^2 r_n)(1 + \gamma r_n^2 + \beta r_n^3)$$

and

$$\beta = \frac{kI}{a^3 t_s}, \qquad \gamma = \frac{EI}{GRa^2}.$$

Equations (11), (12) and (14) suffice to determine the coefficients A_n. For the built-in case we have:

$$A_n = \frac{2(1 + \alpha)\sin r_n}{\alpha D_n}\left\{S_1 + \gamma - \frac{\alpha}{3(1 + \alpha)} + \frac{1}{r_n^2}\right\} \qquad \ldots\ldots\ldots\ldots \quad (15)$$

where

$$S_1 = \frac{\Sigma \frac{\cos^2 r_n}{D_n} \left\{ \gamma - \frac{\alpha}{3(1+\alpha)} + \frac{1}{r_n^2} \right\}}{\frac{1}{2\alpha(1+\alpha)} - \Sigma \frac{\cos^2 r_n}{D_n}} \quad \ldots \quad \ldots \quad \ldots \quad \ldots \quad \ldots \quad (15a)$$

If the rib-boom is simply-supported:

$$A_n = \frac{2(1+\alpha)\sin r_n}{\alpha D_n} \left\{ S_2 + \gamma + \frac{1}{3(1+\alpha)} + \frac{1}{r_n^2} \right\} \quad \ldots \quad \ldots \quad \ldots \quad \ldots \quad (16)$$

where

$$S_2 = \frac{-\Sigma \frac{\cos^2 r_n}{D_n} \left\{ \gamma + \frac{1}{3(1+\alpha)} + \frac{1}{r_n^2} \right\}}{\frac{1}{2(1+\alpha)} + \Sigma \frac{\cos^2 r_n}{D_n}} \quad \ldots \quad \ldots \quad \ldots \quad \ldots \quad \ldots \quad (16a)$$

The complete solution to the problem has now been obtained and expressions for the stresses can be written down. But equations (15), (15a), (16) and (16a) are quite unsuited as they stand because of small differences which occur in the computation which necessitate extraordinary accuracy. However, by using the identities given in Ref. 5:

$$\left.\begin{aligned} \Sigma \frac{1}{r_n^2} &\equiv \frac{1+3\alpha}{6(1+\alpha)}, \\ \Sigma \frac{1}{\left(\frac{1+\alpha}{\alpha^2}\right) + r_n^2} &\equiv \frac{\alpha}{2(1+\alpha)}, \end{aligned}\right\} \quad \ldots \quad \ldots \quad \ldots \quad \ldots \quad \ldots \quad (17)$$

we can transform these equations and make them suitable for computation, as well as simplifying them.

It is convenient to introduce the following additional notation:

$$\left.\begin{aligned} T &= \Sigma \frac{r_n \sin^2 r_n}{D_n} \\ U &= \Sigma \frac{\sin^2 r_n}{D_n} \\ V &= \Sigma \frac{\sin^2 r_n}{r_n D_n} \\ W &= \Sigma \frac{\sin^2 r_n}{r_n^2 D_n} \\ &\equiv \frac{\alpha}{2(1+\alpha)} - \beta T - \gamma U, \end{aligned}\right\} \quad \ldots \quad \ldots \quad \ldots \quad \ldots \quad \ldots \quad (18)$$

$$X_1 = S_1 + \gamma - \frac{\alpha}{3(1+\alpha)}$$
$$X_2 = S_2 + \gamma + \frac{1}{3(1+\alpha)}$$
} constant terms occurring in equations (15) and (16) .. .. (19)

Expressions for the X's now become

$$X_1 = \gamma - \frac{\beta V}{\gamma U + \beta T},$$
$$= -V/T \text{ if } \gamma \text{ is zero,}$$
.. .. (19a)

and

$$X_2 = \gamma + \frac{\beta V}{\frac{\alpha^2}{2(1+\alpha)} + W}.$$ .. .. (19b)

These expressions for X_1 and X_2 do not involve small differences of relatively large numbers and are, therefore, not sensitive to small inaccuracies in the r_n (or allied functions).

The direct stress in the spar flanges is now given by

$$\frac{\sigma_F}{f} = 1 + \frac{2(1+\alpha)}{\alpha^2} \Sigma \frac{\sin^2 r_n}{D_n} \left\{X + \frac{1}{r_n^2}\right\} \exp\left(\frac{-r_n x}{ak}\right)$$

and the shear stress adjacent to the spar flanges by

$$\frac{\tau}{f_0} = -2\left(\frac{Gt_s}{Et}\right)^{1/2} \Sigma \frac{r_n \sin^2 r_n}{D_n} \left\{X + \frac{1}{r_n^2}\right\} \exp\left(\frac{-r_n x}{ak}\right).$$

If the rib-boom is built-in it will be found that:

the proportion of total direct load transferred by the rib-boom is

$$\frac{2\beta}{\alpha}\left\{T + \frac{UV}{\beta T + \gamma U}\right\},$$

the shear stress at the root adjacent to the spar flanges is given by

$$\frac{-\tau}{f_0} = 2\gamma \left(\frac{Gt_s}{Et}\right)^{1/2} \left\{T + \frac{UV}{\beta T + \gamma U}\right\},$$

and the bending-moment in the rib-boom at its ends is given by

$$\frac{M}{f_0 a^2 t_s} = \frac{\beta V}{\beta T + \gamma U}.$$

If the rib-boom is simply-supported:

the proportion of total direct load transferred by the rib-boom is

$$\frac{2\beta}{\alpha}\left\{T - \frac{UV}{\frac{\alpha}{2} - \beta T - \gamma U}\right\},$$

and the shear stress at the root adjacent to the spar flanges is given by

$$\frac{-\tau}{f_0} = 2\left(\frac{Gt_s}{Et}\right)^{1/2}\left\{V + \gamma T + \frac{\beta TV}{\frac{\alpha}{2} - \beta T - \gamma U}\right\}$$

$$= 2\left(\frac{Gt_s}{Et}\right)^{1/2}\left(\frac{V}{\frac{1}{2} - \frac{\beta T}{\alpha}}\right) \quad \text{if } \dot{\gamma} \text{ is zero.}$$

Tables of T, U, V for various α, β and γ

$\alpha = \frac{1}{2}$, $\gamma = 0$

β	10^{-5}	5×10^{-5}	2×10^{-4}	8×10^{-4}	32×10^{-4}
T	825	280·4	109·9	42·49	16·09
U	16·97	9·508	5·670	3·282	1·818
V	0·9707	0·8004	0·6559	0·5148	0·3804

$\gamma = 0{\cdot}04\beta^{1/2}$

$\alpha = 1$

β	5×10^{-5}	2×10^{-4}	8×10^{-4}	32×10^{-4}
T	264·4	105·9	42·12	16·56
U	9·414	5·827	3·563	2·099
V	0·9473	0·8054	0·6648	0·5253

$\alpha = 1$, $\gamma = 0$

β	5×10^{-5}	2×10^{-4}	8×10^{-4}	32×10^{-4}
T	282·5	111·7	43·93	17·14
U	9·962	6·104	3·681	2·167
V	0·9718	0·8255	0·6801	0·5370

$\alpha = 2$, $\gamma = 0$

β	5×10^{-5}	2×10^{-4}	8×10^{-4}	32×10^{-4}
T	283·2	112·3	44·47	17·58
U	10·20	6·337	3·905	2·377
V	1·105	0·9577	0·8111	0·6651

APPENDIX II

Effect of Rotation of the Spar Flanges

When the rib-boom is built-in the end-moments will be slightly relieved due to the rotation of the spar flanges. This reduction in the end-moments may be estimated by the following analysis. Throughout γ is taken as zero.

The rotational stiffnesses K_F and K_R of the spar flange and rib-boom will be determined. A pin-jointed connection between rib-boom and spar flange is assumed and the spar flange is treated 'as a beam' on an elastic foundation.

The following additional notation is employed:

v		Deflection of the spar flange in the y-direction
EI_F		Flexural stiffness of spar flange
t_r		Effective thickness of skin and ribs in carrying direct load in the y-direction
F_R		Section area of rib-boom
λ	$=$	$(t_r/4aI_F)^{1/4}$
K_F		Rotational stiffness of the spar flange, *i.e.*, Moment required to produce unit dv/dx of spar flange
K_R		Rotational stiffness of the rib-boom, *i.e.*, Moment required to produce unit du/dy of rib-boom

From symmetry, v is zero midway between the two spar flanges and so the lateral load per unit length applied to the spar flange is Evt_r/a. The differential equation for v may now be written

$$\frac{d^4v}{dx^4} + 4\lambda^4 v = 0$$

so that the solution is of the form

$$v = e^{-\lambda x}(A \sin \lambda x + B \cos \lambda x).$$

A relation between A and B is found from the condition of equilibrium of the spar flange and thence it is found that

$$K_F = \lambda EI_F \left(\frac{t_r + 2\lambda F_R}{t_r + \lambda F_R}\right). \quad .. \quad .. \quad .. \quad .. \quad .. \quad .. \quad (20)$$

K_R may be found simply by observing that the end-moment obtained for the built-in case is just sufficient to cause a rotation equal to the shear strain for the simply-supported case, so that

$$K_R = a^2 \sqrt{(EGtt_s)} \left(\frac{1}{2T} - \frac{\beta}{\alpha}\right). \quad .. \quad .. \quad .. \quad .. \quad .. \quad .. \quad (21)$$

Due to the rotation of the spar flanges the bending-moment for the built-in case will be reduced in the ratio

$$K_F \ : \ (K_F + K_R) \quad .. \quad .. \quad .. \quad .. \quad .. \quad .. \quad .. \quad (22)$$

For example with the structure as in Section 6 if we take

$$t_r = t = 0{\cdot}05 \text{ in.}$$
$$I_F = 25 \text{ in.}^4$$

it will be found that

$$\lambda = 0{\cdot}0563$$

so that

$$K_F = 2{\cdot}29E.$$

From equation (21) $K_R = 0{\cdot}556E$

Therefore

$$\frac{K_F}{K_F + K_R} = 80 \text{ per cent.}$$

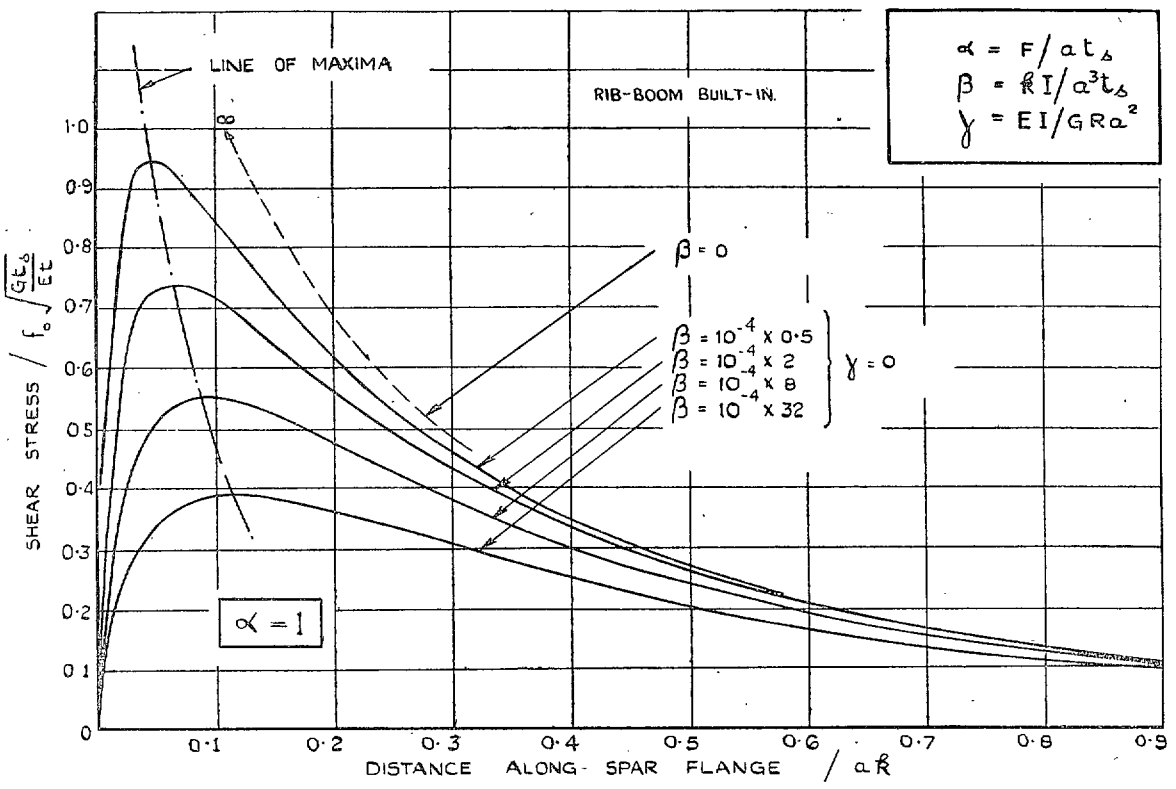

FIG. 1. Shear stress adjacent to spar flange (shear flexibility of rib-boom ignored).

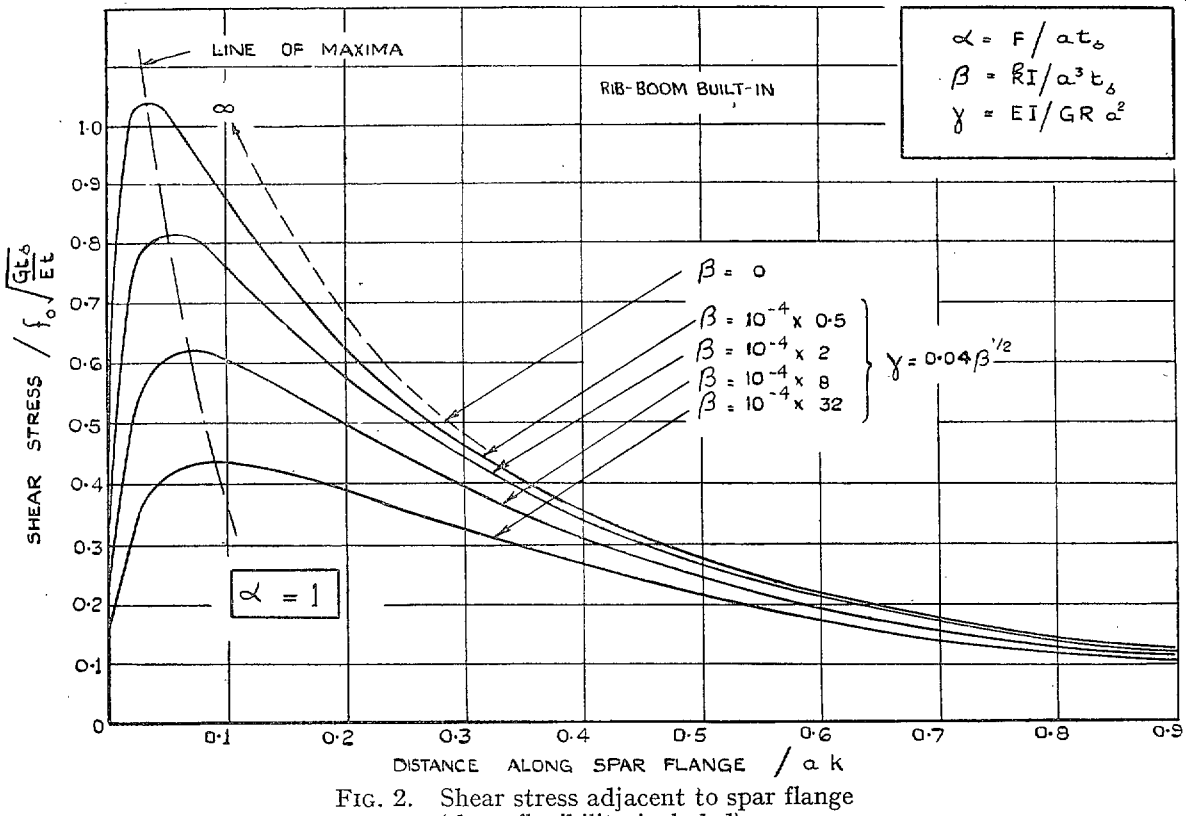

FIG. 2. Shear stress adjacent to spar flange (shear flexibility included).

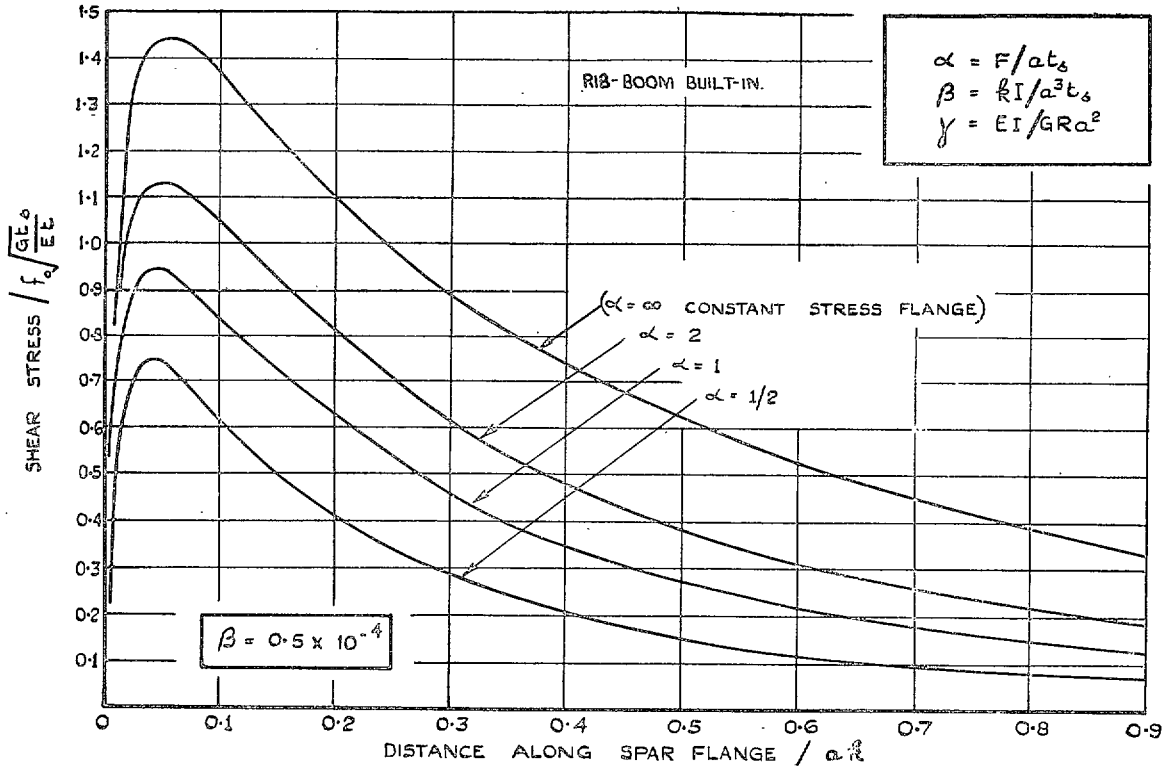

FIG. 3. Shear stress adjacent to spar flange
(effect of increasing flange area).

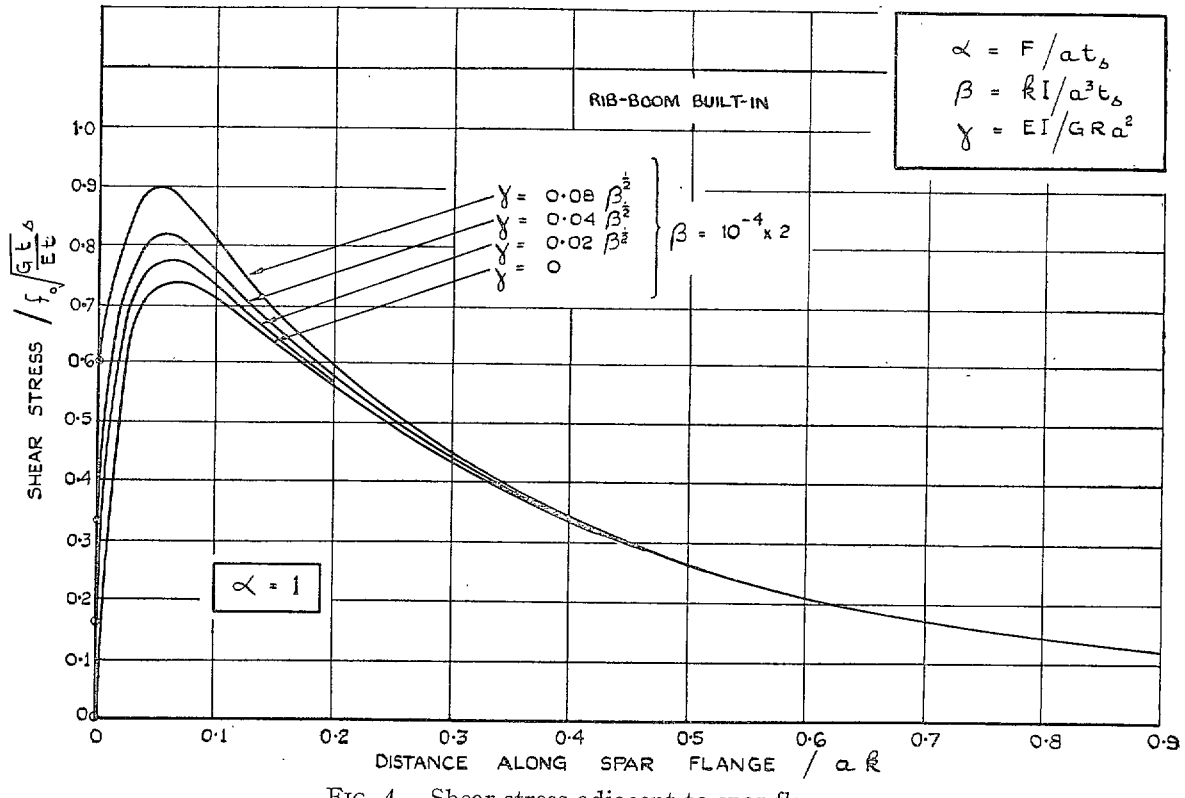

FIG. 4. Shear stress adjacent to spar flange
(effect of varying shear flexibility of rib-boom).

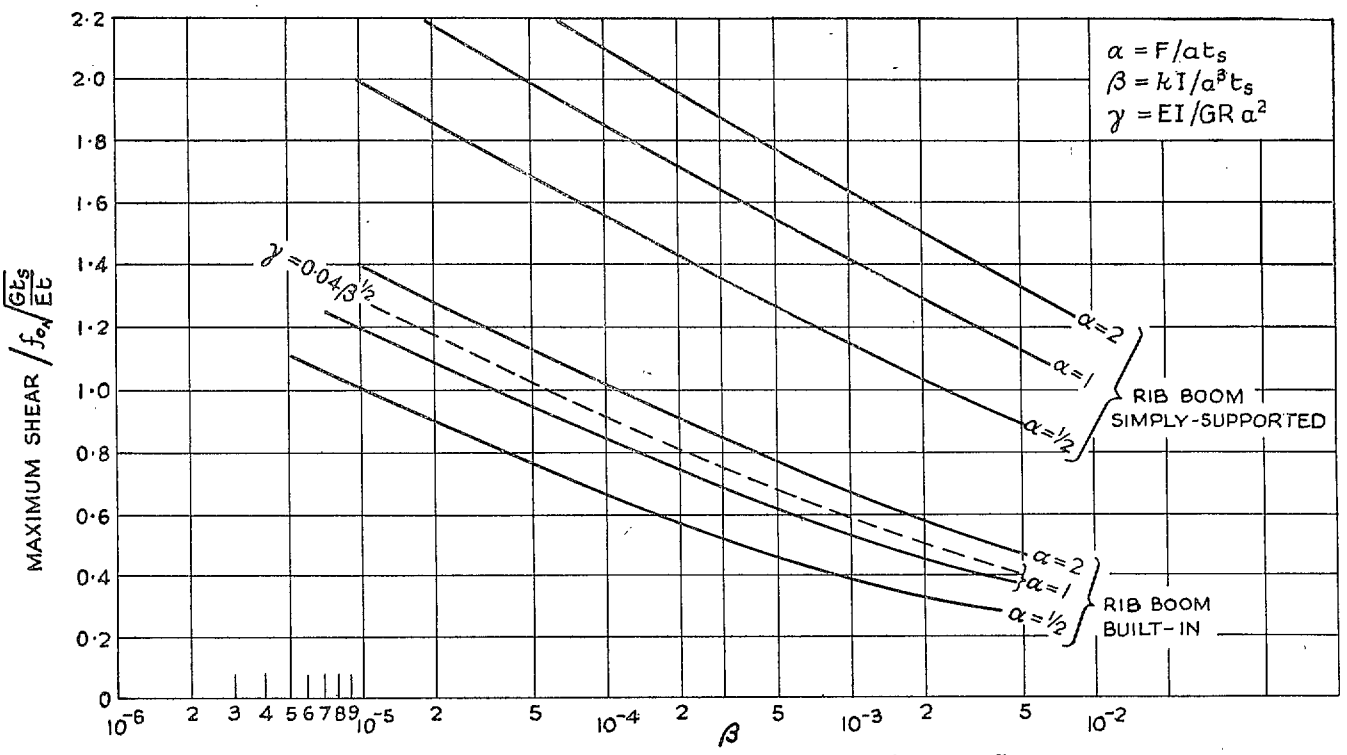

FIG. 5. Peak values of shear stress adjacent to the spar flanges.

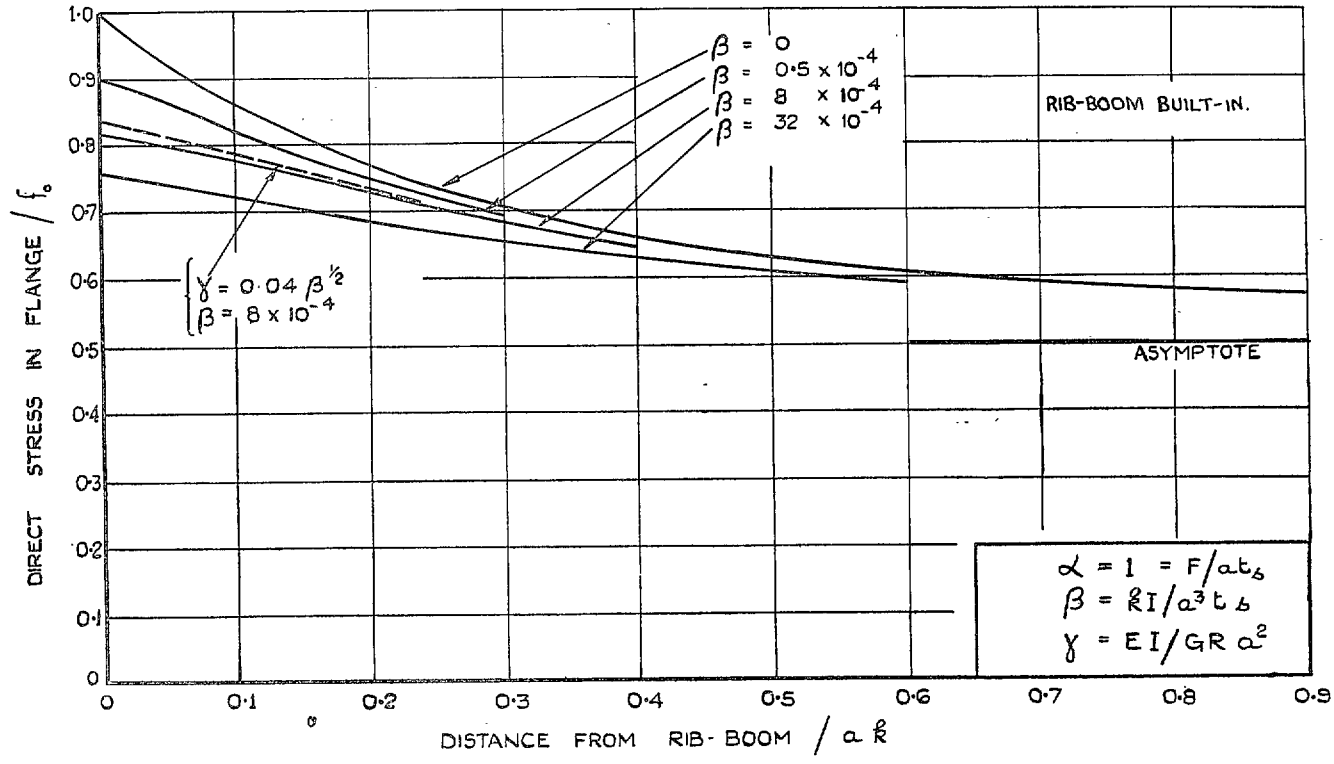

FIG. 6. Distribution of direct stress in the spar flanges.

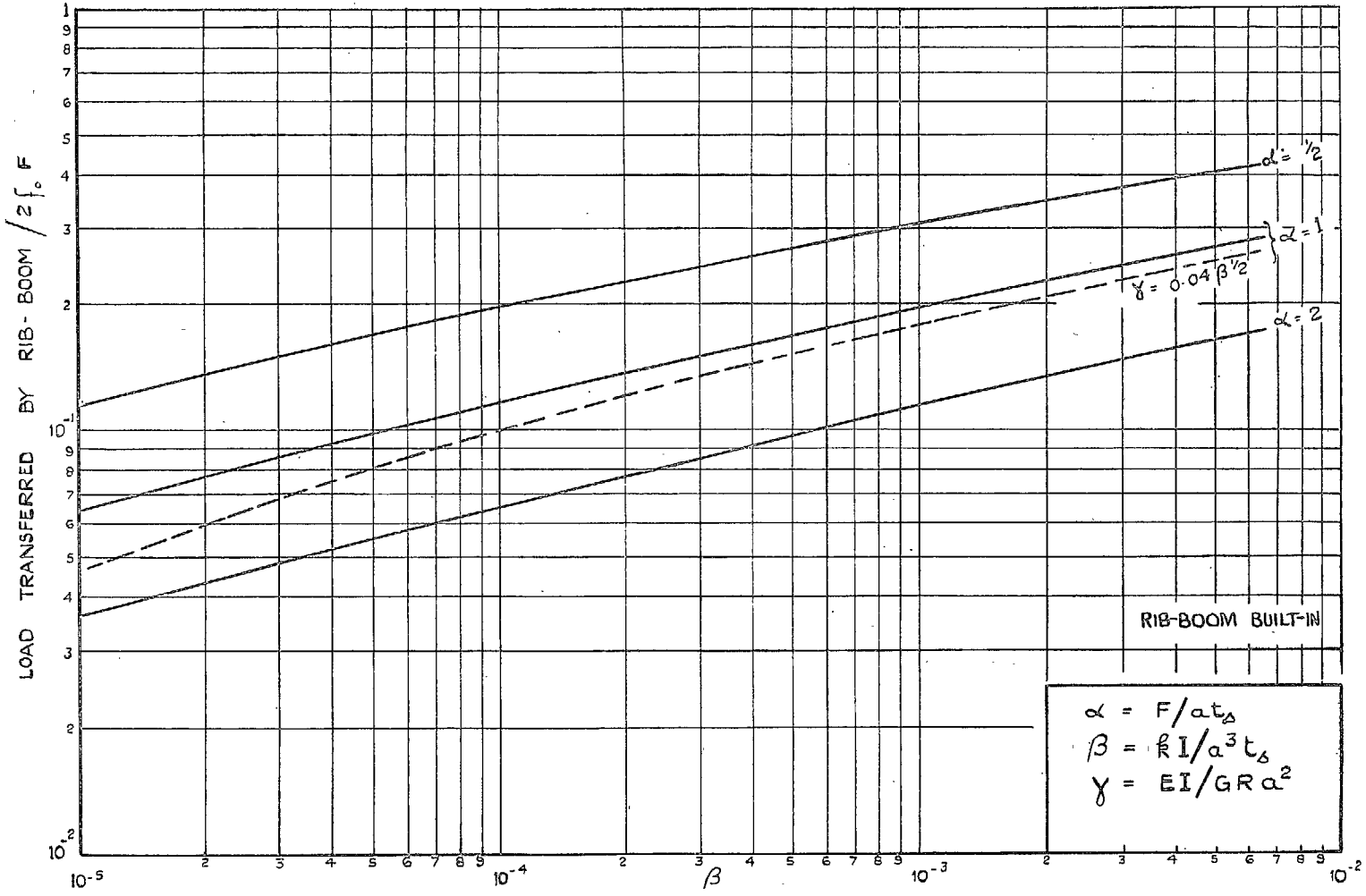

FIG. 7. Proportion of total load transferred by rib-boom.

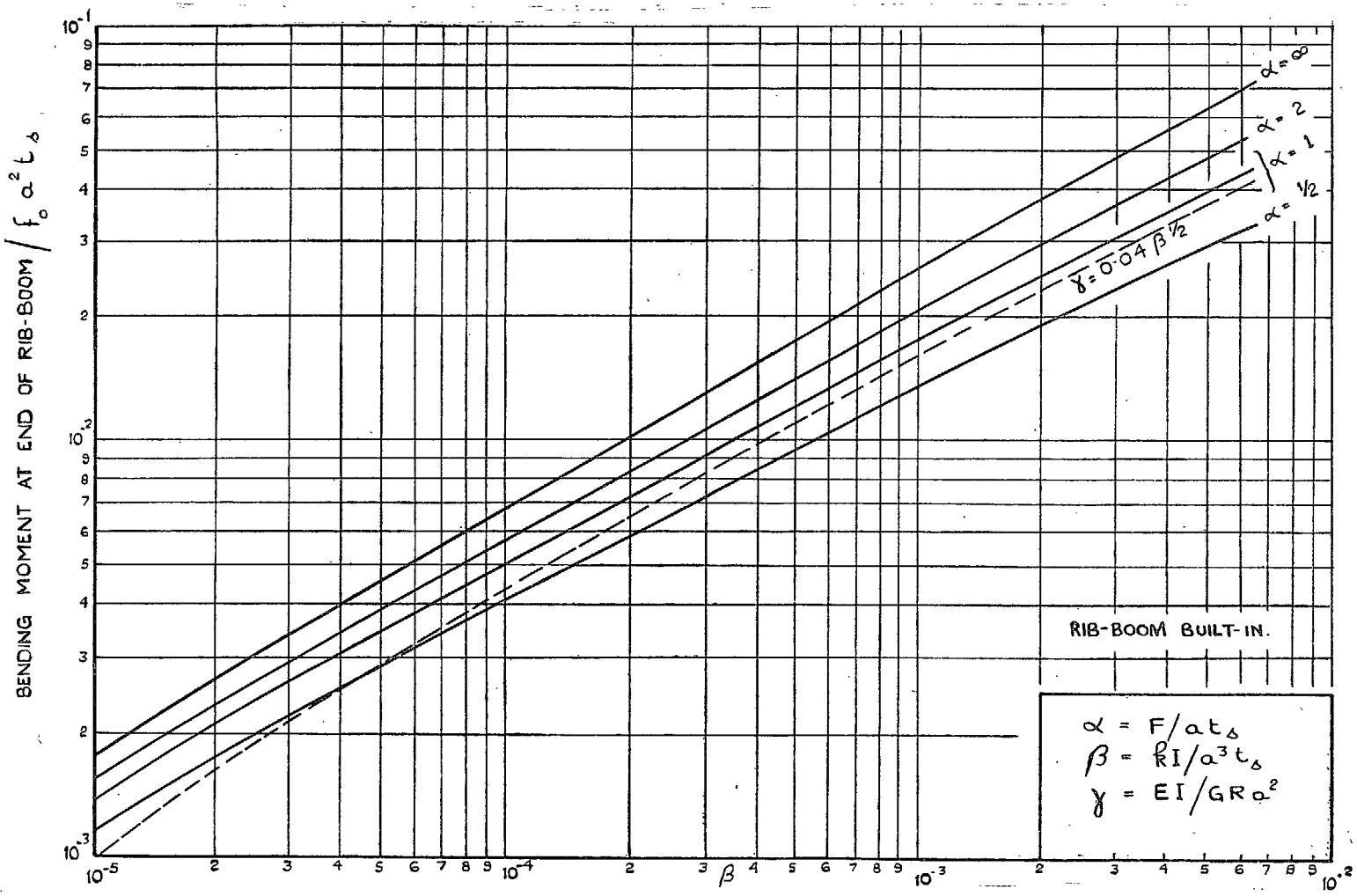

FIG. 8. Bending-moment at end of rib-boom.

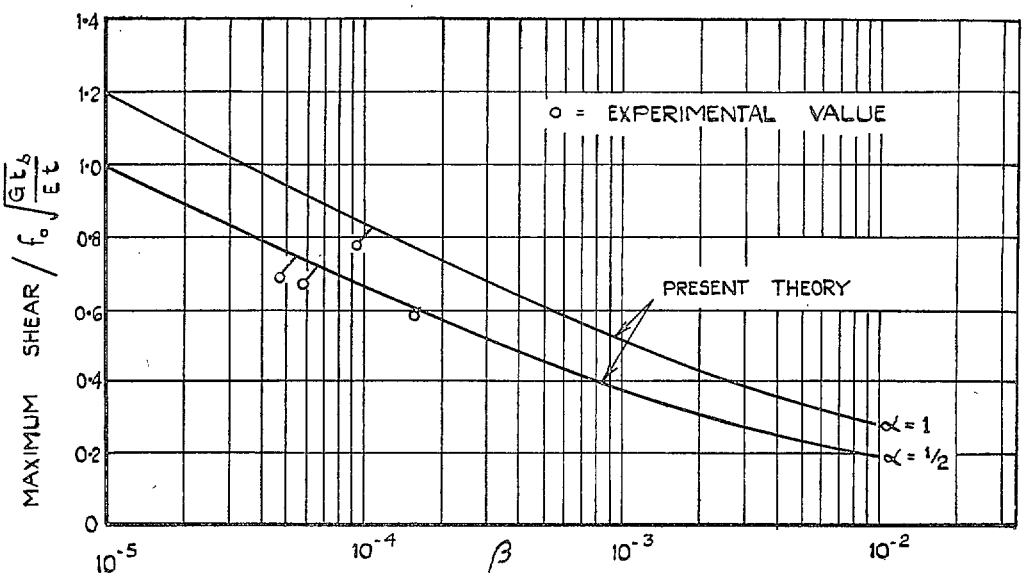

FIG. 9a. Maximum shear stresses.

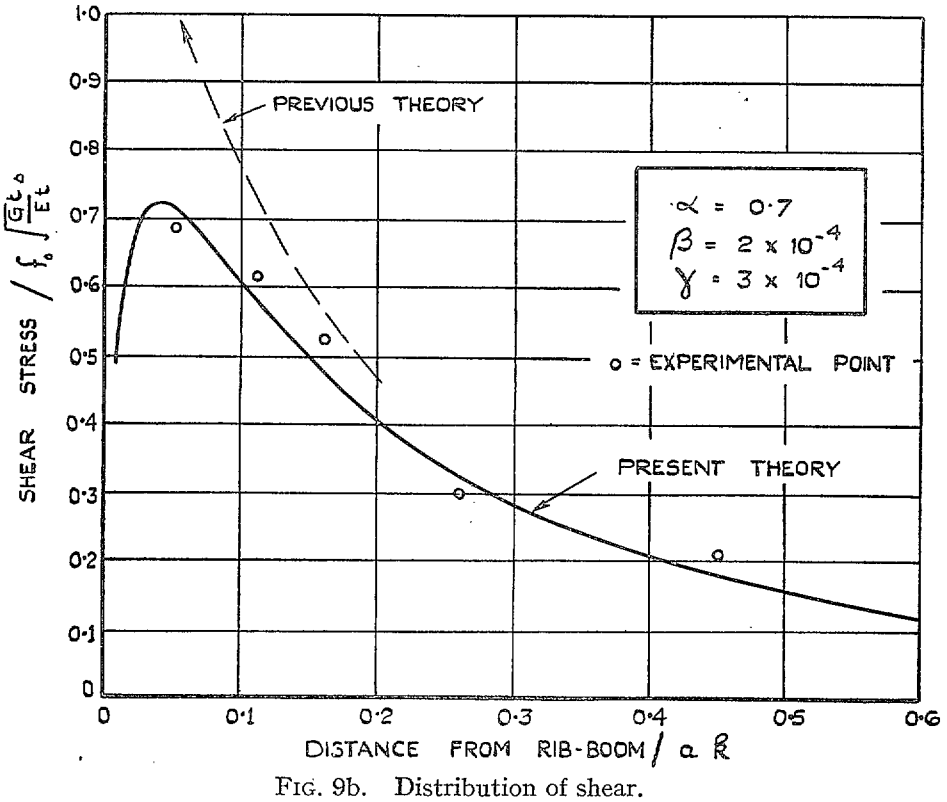

FIG. 9b. Distribution of shear.
Agreement with experiment.

(935) Wt.15 K9 12/52 H.P.Co. 34/261

PRINTED IN GREAT BRITAIN

Publications of the Aeronautical Research Council

ANNUAL TECHNICAL REPORTS OF THE AERONAUTICAL RESEARCH COUNCIL (BOUND VOLUMES)—

1934–35 Vol. I. Aerodynamics. *Out of print.*
Vol. II. Seaplanes, Structures, Engines, Materials, etc. 40*s.* (40*s.* 8*d.*)

1935–36 Vol. I. Aerodynamics. 30*s.* (30*s.* 7*d.*)
Vol. II. Structures, Flutter, Engines, Seaplanes, etc. 30*s.* (30*s.* 7*d.*)

1936 Vol. I. Aerodynamics General, Performance, Airscrews, Flutter and Spinning. 40*s.* (40*s.* 9*d.*)
Vol. II. Stability and Control, Structures, Seaplanes, Engines, etc. 50*s.* (50*s.* 10*d.*)

1937 Vol. I. Aerodynamics General, Performance, Airscrews, Flutter and Spinning. 40*s.* (40*s.* 10*d.*)
Vol. II. Stability and Control, Structures, Seaplanes, Engines, etc. 60*s.* (61*s.*)

1938 Vol. I. Aerodynamics General, Performance, Airscrews. 50*s.* (51*s.*)
Vol. II. Stability and Control, Flutter, Structures, Seaplanes, Wind Tunnels, Materials. 30*s.* (30*s.* 9*d.*)

1939 Vol. I. Aerodynamics General, Performance, Airscrews, Engines. 50*s.* (50*s.* 11*d.*)
Vol. II. Stability and Control, Flutter and Vibration, Instruments, Structures, Seaplanes, etc. 63*s.* (64*s.* 2*d.*)

1940 Aero and Hydrodynamics, Aerofoils, Airscrews, Engines, Flutter, Icing, Stability and Control, Structures, and a miscellaneous section. 50*s.* (51*s.*)

Certain other reports proper to the 1940 *volume will subsequently be included in a separate volume.*

ANNUAL REPORTS OF THE AERONAUTICAL RESEARCH COUNCIL—

1933–34	1*s.* 6*d.* (1*s.* 8*d.*)
1934–35	1*s.* 6*d.* (1*s.* 8*d.*)
April 1, 1935 to December 31, 1936.	4*s.* (4*s.* 4*d.*)
1937	2*s.* (2*s.* 2*d.*)
1938	1*s.* 6*d.* (1*s.* 8*d.*)
1939–48	3*s.* (3*s.* 2*d.*)

INDEX TO ALL REPORTS AND MEMORANDA PUBLISHED IN THE ANNUAL TECHNICAL REPORTS, AND SEPARATELY—

April, 1950 — R. & M. No. 2600. 2*s.* 6*d.* (2*s.* 7½*d.*)

INDEXES TO THE TECHNICAL REPORTS OF THE AERONAUTICAL RESEARCH COUNCIL—

December 1, 1936 — June 30, 1939.	R. & M. No. 1850.	1*s.* 3*d.* (1*s.* 4½*d.*)
July 1, 1939 — June 30, 1945.	R. & M. No. 1950.	1*s.* (1*s.* 1½*d.*)
July 1, 1945 — June 30, 1946.	R. & M. No. 2050.	1*s.* (1*s.* 1½*d.*)
July 1, 1946 — December 31, 1946.	R. & M. No. 2150.	1*s.* 3*d.* (1*s.* 4½*d.*)
January 1, 1947 — June 30, 1947.	R. & M. No. 2250.	1*s.* 3*d.* (1*s.* 4½*d.*)

Prices in brackets include postage.

Obtainable from

HER MAJESTY'S STATIONERY OFFICE

York House, Kingsway, LONDON, W.C.2 — 423 Oxford Street, LONDON, W.1
P.O. Box 569, LONDON, S.E.1
13a Castle Street, EDINBURGH, 2 — 1 St. Andrew's Crescent, CARDIFF
39 King Street, MANCHESTER, 2 — Tower Lane, BRISTOL, 1
2 Edmund Street, BIRMINGHAM, 3 — 80 Chichester Street, BELFAST

or through any Bookseller

S.O. Code No. 23-2663